JACC Vol. 30, No. 2
August 1997:585–91

Extension of Hemorrhage After Reperfusion of Occluded Coronary Artery: Contrast Echocardiographic Assessment in Dogs

TOSHIAKI SHISHIDO, MD, SHINTARO BEPPU, MD, FACC,* HISAO MATSUDA, MD, CHIKAO YUTANI, MD, KUNIO MIYATAKE, MD, FACC

Osaka, Japan

Objectives. **The aim of this study was to elucidate the progression of intramural hemorrhage complicated by reperfusion with the use of myocardial contrast echocardiography.**

Background. **Although hemorrhagic infarction is known to occur in ischemia followed by reperfusion, its onset and sequence have not been well characterized.**

Methods. **In 20 anesthetized dogs, 3-h occlusion of the left circumflex coronary artery was followed by reperfusion. The area at risk during coronary occlusion was ~25%. Myocardial contrast echocardiogram was examined, and the time-intensity curves for both ischemic and nonischemic areas were obtained at baseline, at 3 min after reperfusion and then at 15-min intervals until 90 min after reperfusion. The wall thickness of both areas was also measured.**

Results. **Gross hemorrhage in the reperfused areas was observed in five dogs (Group H) but not in seven dogs (Group NH). All wall segments were opacified at 3 min after reperfusion in both groups. However, the contrast defect spread significantly with time after reperfusion in Group H but not in Group NH (18.7 ± 3.4% and 3.3 ± 1.8%, respectively, at 90 min after reperfusion $p < 0.005$). The wall of the risk area at 90 min after reperfusion had thickened to 1.3 times baseline thickness in Group H but was unchanged in Group NH. The other eight dogs were excluded from study because of fatal arrhythmias or the existence of collateral circulation during coronary occlusion.**

Conclusions. **Both progression of the contrast defect area on myocardial contrast echocardiography and a gradual thickening of the wall with reperfusion are characteristic of hemorrhagic infarction.**

(J Am Coll Cardiol 1997;30:585–91)

Reperfusion in the early stages of myocardial infarction (MI) is an indispensable part of therapy directed to relieving the oxygen deficits of viable cardiac myocytes in ischemic areas. However, reperfusion of an artery supplying an infarct area may also cause irreversible damage to viable myocytes in some cases. This phenomenon is called *reperfusion injury* (1–11). Hemorrhagic MI, which retards the healing process after infarction, is also a type of reperfusion injury (12). Hemorrhagic MI occurs after prolonged ischemia followed by reperfusion in experimental models (1,12–17) and even in 20% of clinical patients (1). However, its clinical significance has not been determined because its onset and progression of extension cannot be diagnosed.

Radionuclide examination, which allows a nonreperfused bed to be identified accurately, is not suitable for detecting infarct extension within a few hours in a reperfused bed. For this reason, myocardial contrast echocardiography (MCE) is a preferable method for directly and repeatedly visualizing an area of a reperfused vascular bed (18–21). MCE demonstrates the area with microvasculature intact. More precisely, the opacified area identified by MCE represents the functional territory of the coronary artery, without regard for occluded branches, presence of collateral vessels or form of complex bifurcation (18–23). Moreover, wall motion and thickening can be analyzed simultaneously by MCE. We studied the progression of hemorrhagic MI in dogs with prolonged coronary occlusion followed by reperfusion, examining sequential changes in abnormal wall thickening and the contrast-opacified areas, as well as the areas of hemorrhage in postmortem specimens.

Methods

Animal preparation. Twenty mongrel dogs weighing 16 ± 3 kg (mean ± SD) were anesthetized with intravenous sodium pentobarbital (30 mg/kg body weight intravenously, Abbott Laboratories) after premedication with ketamine hydrochloride (5 mg/kg intramuscularly, Sankyo Co., Tokyo, Japan). The study conformed to the "Position of the American Heart Association on Research Animal Use" adopted November 11, 1984 by the American Heart Association. The dogs were intubated, and ventilated through use of a respirator pump

From the Department of Cardiovascular Dynamics, Department of Pathology and Cardiology Division of Medicine, National Cardiovascular Center Research Institute; and *School of Allied Health Sciences, Faculty of Medicine, Osaka University, Suita, Osaka, Japan. This study was supported by Grants-in Aid for Scientific Research (A) (No. 07557344) from the Ministry of Education, Science, Sports and Culture of Japan, Tokyo, Japan.

Manuscript received September 11, 1996; revised manuscript received April 2, 1997, accepted April 16, 1997.

Address for correspondence: Dr. Toshiaki Shishido, Department of Cardiovascular Dynamics, National Cardiovascular Center Research Institute, 5-7-1 Fujishirodai, Suita, Osaka 565, Japan. E-mail: tosjoe@ri.ncvc.go.jp.

0735-1097/97/$17.00
PII S0735-1097(97)00163-0

Abbreviations and Acronyms

CBF = coronary blood flow
LCx = left circumflex coronary artery
MCE = myocardial contrast echocardiography or echocardiogram
MI = myocardial infarction
PI = peak intensity above baseline intensity

(model Mark 7, Bird). Additional anesthesia was administered during the experiment as needed. A 7F catheter was placed in the descending thoracic aorta by way of the right femoral artery for recording of systemic blood pressure and measurement of blood gases. A similar catheter was placed in the right femoral vein for administration of fluids and drugs as needed. A 6F catheter with a side hole was placed in the left coronary sinus of Valsalva to inject a contrast agent for MCE.

The dogs were then placed in the right lateral decubitus position and their chest was opened along the fourth or fifth intercostal space. The pericardium was incised and used as a cradle for the exposed heart. A microtipped pressure transducer (model SPC-350, Millar) was inserted into the left ventricular cavity by way of the left ventricular apex. The proximal left anterior descending coronary artery (LCx) was dissected free from surrounding tissues, and an ultrasound flow probe (model 4RS, Transonic Systems Inc.) was placed around it to monitor the epicardial coronary blood flow (CBF). A polyethylene capillary tube placed proximal to the flow probe at the LCx was used to produce coronary occlusion. An initial bolus injection of heparin (50 U/kg) administered intravenously after insertion of these catheters was followed every hour by supplemental injections of half the bolus amount to prevent clotting of the catheter side holes.

Contrast agent preparation. A sonicator (model 250, Branson) with a 3-mm diameter horn was used to generate microbubbles. Ten milliliters of 5% human albumin (Green Cross, Osaka, Japan) was sonicated for 30 s in an outer tube of a 20-ml syringe. The power of the sonicator was 20 W and the frequency 20 kHz. After 10 s of elapsed time to avoid contamination from relatively large microbubbles, 2 ml of the contrast solution was withdrawn to a syringe and 1 ml was injected manually as a bolus with a speed of 1 ml/s. This method produced a stable echocardiographic contrast agent containing microbubbles 11 ± 12 μm (median 5 μm) in diameter and 3.9×10^5/ml in density, which were measured by Coulter counter ZM (Coulter Corp.).

MCE. The echocardiographic system used was a phased array system (SSH-60A, Toshiba, Tokyo, Japan) with a 3.5-MHz transducer. Image registration was set to provide a short-axis view at the midpapillary muscle level. The transducer was placed directly on the epicardial surface of the heart such that the posterior wall was perpendicular to the ultrasound beam. Newly developed asynergy of the posterior wall was examined by transient occlusion of the LCx. Gain settings were optimized initially and held constant throughout the experiment. Sonicated albumin microbubbles were injected into the left coronary sinus of Valsalva during echocardiographic recording. The respirator was kept off until the myocardial opacification disappeared in order to fix the heart position in the echocardiographic image. The images were recorded on S-VHS videotape with use of a high fidelity video recorder (model AG-7300, Panasonic, Osaka, Japan).

An off-line image analysis system (Color Cardiology Work Station, Freeland Systems) was used to measure myocardial videointensity by using a scale from black to white containing 256 shades of gray. Every end-diastolic frame from the time of contrast injection until disappearance of myocardial opacification was stored in this system. Regions of interest were placed at the center of the ventricular septum as a control area, and at the center of the posterior wall, which showed a contrast defect during coronary occlusion. Both regions were rectangular with dimensions of $\sim 7 \times 15$ mm. From time-videointensity curves from each region of interest, baseline and peak intensities were measured. Peak intensity above baseline intensity is referred to simply as *peak intensity (PI)* in this study.

As shown in the results, hemorrhage was found mainly on the endocardial side of the ventricular wall. The posterior wall was divided into three regions: endocardial, mid- and epicardial layers, in each of which time-intensity curves were also examined.

Echocardiographic measurement. The left ventricular end-diastolic and end-systolic diameter and the wall thickness of the anterior (or ventricular septum) and posterior walls of the left ventricle were measured from M-mode echocardiograms in the standard manner. Systolic thickening of the ventricular wall was calculated as (Systolic wall thickness − Diastolic wall thickness)/Diastolic wall thickness. We also calculated the wall thickness ratio by dividing the end-diastolic thickness of the posterior wall by that of the anterior or septal wall, to avoid the influence of loading conditions. When the posterior wall is thickened, this ratio is larger than the baseline value.

Experimental protocol. Baseline images from MCE were obtained after confirming the absence of regional wall motion abnormalities and the presence of good and homogeneous opacification of the entire left ventricular wall. After administration of lidocaine (1.5 mg/kg intravenously), the LCx was occluded for 180 min. The ultrasound flow meter signal was used to verify complete coronary occlusion during this period. At 15 and 180 min after occlusion, MCE was performed to examine the contrast defect area. When the contrast defect area decreased during coronary occlusion, the dog was excluded from the study because of the existence of collateral circulation. After 3 h of occlusion, lidocaine (1.5 mg/kg intravenously) was again administered, and the coronary occlusion was released. MCE was performed just before release of the occlusion, and at 3, 15, 30, 60 and 90 min after reperfusion. The epicardial CBF of the LCx, aortic and left ventricular pressures and heart rate were continuously monitored throughout the experiment.

Postmortem examination. The dog's heart was excised and cut in 1-cm thick slices along the short axis from the apex to the base to examine for the presence of gross hemorrhage affecting the ventricular wall. After fixation in 10% formalin, these slices were photographed (35-mm film). The total myocardial areas and hemorrhagic areas were calculated by digitization of these photographs by using a commercially available Macintosh-based computer system with the public domain NIH IMAGE computer-assisted digital imaging processor. The hemorrhagic area was expressed as a percent of total myocardial area. The area attributable to the papillary muscles was not included.

The slices were stained with hematoxylin-eosin to microscopically examine infarct areas. The area of MI was defined as the region that included coagulation necrosis, contraction band necrosis, wavy change of myofibrils, margination of neutrophils, pyknotic nuclei and edema of the interstitium, excluding the area containing a mixture of normal and necrotic cells at the border of the infarct area (24). Photomicrographs were taken of the slices and traced for determination of infarct size.

Statistical analysis. Variables are presented as the mean value ± SD. Two-way repeated measures analysis of variance with the Newman-Keuls test was applied for multiple comparison under reperfusion conditions. The correlation was assessed by linear regression analysis with use of a least-squares method. A p value < 0.05 was considered significant.

Results

The entire protocol could be completed in 12 of the 20 dogs. Eight dogs did not complete the protocol because of the existence of collateral circulation (n = 3) or fatal arrhythmia immediately after coronary occlusion or reperfusion (n = 5). Gross hemorrhage was observed in five dogs. The area of hemorrhage ranged from 19.3% to 26.7% of the total myocardial cross-sectional area. Figure 1 shows a representative hemorrhagic case. In the remaining seven dogs, there was no macroscopic hemorrhage, whereas some extravasation of erythrocytes into the myocardial interstitium could be found on histologic examination. In the results that follow, the analyzed data are compared between the dogs with (Group H) and without (Group NH) gross (macroscopic) hemorrhage.

Hemodynamic variables. There was no significant change in heart rate, mean aortic pressure, left ventricular end-diastolic pressure or peak positive first derivative of left ventricular pressure after reperfusion in either group (Table 1). In both groups, epicardial CBF of the LCx increased to 240% of baseline value immediately after reperfusion, followed by a gradual decline of flow to 50% to 70% of baseline value. Thus, hemodynamic changes after reperfusion did not differ between the two groups.

Systolic thickening and wall thickness. In Group NH, systolic thickening of the posterior wall was 38.3 ± 11.1% at baseline and 6.2 ± 9.0% at 3 min after reperfusion (Fig. 2A); the systolic thickening recovered gradually and was 17.1 ± 11.9% at 90 min after reperfusion. In Group H, systolic thickening of the posterior wall was 33.1 ± 5.6% at baseline and 7.5 ± 6.2% at 3 min after reperfusion. In the reperfusion period, the systolic thickening of the posterior wall did not recover but decreased, even at 90 min after reperfusion (2.5 ± 2.1%, p = NS vs. 3 min after reperfusion). Differences of recovery of systolic thickening at 30, 60 and 90 min after reperfusion were all significantly different between the two groups.

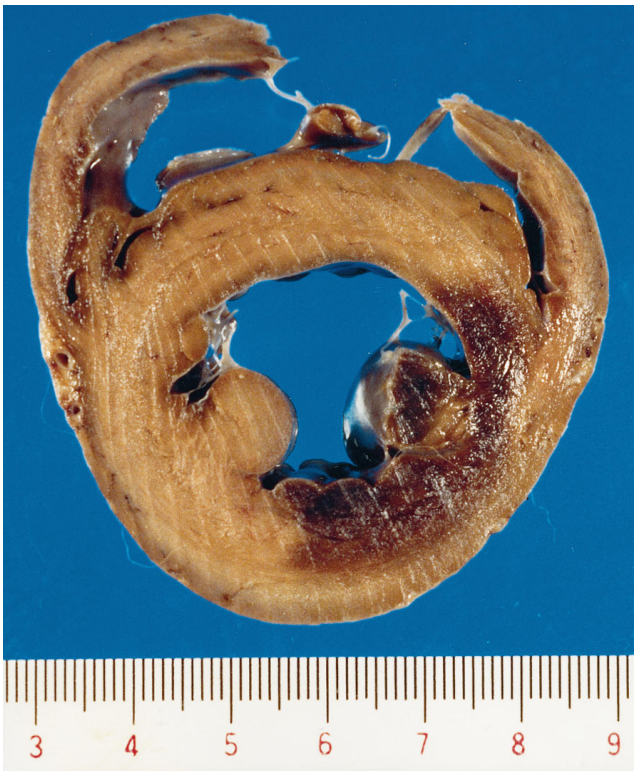

Figure 1. Photograph of a horizontal section of the heart from a representative dog in Group H. Gross hemorrhage occupies a large part of the region of distribution of the LCx.

The wall thickness ratio of posterior to septal wall at end-diastole, in Group NH, was 1.11 ± 0.16 at baseline, 0.86 ± 0.13 before reperfusion, 1.23 ± 0.14 at 3 min after reperfusion and 1.09 ± 0.07 at 90 min after reperfusion (Fig. 2B). Changes in the thickness ratio in Group H until 3 min after reperfusion were the same as those in Group NH, which were 1.07 ± 0.10 at baseline, 0.88 ± 0.06 before reperfusion and 1.20 ± 0.08 at 3 min after reperfusion. In Group H, the thickness ratio increased gradually, becoming 1.32 ± 0.14 at 90 min after reperfusion ($p < 0.005$ vs. Group NH). It was a characteristic of Group H that the reperfused wall became thicker (+27%) and did not show systolic thickening.

Time course of contrast defect size. The contrast defect area was ~25% of the total cross-sectional area of the left ventricular wall in both groups during coronary occlusion (28.2 ± 4.8% in Group H vs. 24.9 ± 5.4% in Group NH). Figure 3 illustrates the time course of contrast defect size after reperfusion. Immediately after reperfusion, the area that had been a contrast defect area during coronary occlusion was

Table 1. Hemodynamic Variables

	Before Occlusion	During Occlusion		After Reperfusion		
		15 min	180 min	3 min	30 min	90 min
HR (beats/min)						
Group H	149 ± 15	150 ± 15	151 ± 12	141 ± 8	143 ± 10	141 ± 12
Group NH	162 ± 21	160 ± 20	156 ± 22	151 ± 19	149 ± 19	148 ± 19
Mean AoP (mm Hg)						
Group H	115 ± 32	102 ± 28	95 ± 18	95 ± 23	94 ± 23	88 ± 24
Group NH	97 ± 9	94 ± 15	90 ± 20	78 ± 16	85 ± 18	87 ± 17
LVEDP (mm Hg)						
Group H	7 ± 5	14 ± 6	11 ± 3	11 ± 6	11 ± 6	11 ± 7
Group NH	5 ± 3	8 ± 6	6 ± 4	8 ± 4	7 ± 4	7 ± 4
Peak positive LV dP/dt (mm Hg/s)						
Group H	2,036 ± 349	1,612 ± 487	1,496 ± 314	1,340 ± 343	1,400 ± 346	1,300 ± 380
Group NH	2,084 ± 254	1,786 ± 195	1,723 ± 321	1,300 ± 252	1,506 ± 240	1,568 ± 242
CBF of LCx (% of baseline)						
Group H	100	. . .	. . .	246 ± 159	68 ± 27*	51 ± 27*
Group NH	100	. . .	. . .	238 ± 76	82 ± 12*	69 ± 16*

*$p < 0.01$ versus 3 min after reperfusion. AoP = aortic pressure; CBF = coronary blood flow; dP/dt = first derivative of left ventricular pressure; Group H = dogs with hemorrhage; Group NH = dogs without hemorrhage; HR = heart rate; LCx = left circumflex coronary artery; LV = left ventricular; LVEDP = left ventricular end-diastolic pressure; . . . = not detected.

clearly and definitely opacified in both groups. In the following period, however, the contrast defect area showed reappearance and spread in Group H. In this group, the contrast defect size was 1.8 ± 2.7% at 3 min after reperfusion, 10.2 ± 4.5% at 30 min ($p < 0.005$ vs. 3 min after reperfusion) and 18.7 ± 3.4% at 90 min after reperfusion ($p < 0.005$). In Group NH, the contrast defect area did not reappear significantly throughout the reperfusion period and was 3.3 ± 1.8% at 90 min after reperfusion ($p < 0.005$ vs. the value in Group H).

Relation between areas of contrast defect, hemorrhage and infarction. The size of the area of gross hemorrhage was not correlated with infarct size. Intramural hemorrhage detected by microscopy was observed only inside the infarct area. The contrast defect area 90 min after reperfusion correlated with the infarct area ($r = 0.712$, $p = 0.014$), but it was smaller than the infarct area in all subjects (Fig. 4A). However, the contrast defect area was almost the same as the area of hemorrhage, showing good linear correlation ($r = 0.872$, $p = 0.054$; Fig. 4B). Figure 5 shows a representative case from Group H. Moreover, the area of gross hemorrhage agreed approximately with the area of contrast defect geometrically.

PI ratio of endocardial to epicardial layer within the postischemic area. PI was almost the same between the endocardial and the epicardial layers of the posterior wall in the two groups before coronary occlusion; that is, the PI ratio was almost 1.0 (Fig. 6). The PI ratio did not change at 3 min after reperfusion in either group. However, in three of the five dogs in Group H, the endocardial layer was not opacified at 15 min after reperfusion, and in another dog, the endocardial layer became unopacified at 60 min after reperfusion. As a result, the PI ratio of the endocardial to the epicardial layer decreased with time in Group H, whereas the ratio was almost constant in Group NH.

Discussion

Progressive wall thickening as an indicator of hemorrhagic infarction. In the present study, systolic thickening decreased and wall thickness increased at later phases of reperfusion in five dog hearts with hemorrhagic MI. Earlier investigators (25) demonstrated an increase in end-diastolic wall thickness during reperfusion after brief coronary occlusion, and they suggested that this change was related to transient increased coronary blood volume secondary to a reactive hyperemic response to reperfusion. This change was analogous to that in our Group NH. Haendchen et al. (26,27) reported that the ventricular wall became far thicker in a model of longer coronary occlusion and suggested that the causes of this thickening were myocardial edema, intracellular and interstitial swelling, intramural hemorrhage, myocardial contracture and extent of necrosis. This change may be analogous to that in our Group H. In addition, our study indicated that the temporal changes in wall thickness after reperfusion were quite different between the two groups. In Group H, the walls thickened in response to reactive hyperemia became progressively thicker despite a lessening of reactive hyperemia, whereas in Group NH the thickened wall returned to normal thickness over time. We conjecture that the progressive thickening of infarct areas after reperfusion is one of the most important diagnostic signs of hemorrhage.

Development of contrast defect after reperfusion as an indicator of hemorrhagic infarction. MCE demonstrates the area of perfused myocardium (18,21,22) and showed that the extent of ischemia during coronary occlusion was almost the same in both Group H and Group NH. After reperfusion, the contrast defect area at 3 min was somewhat smaller than that at 15 min in both groups. Villanueva and co-workers (28)

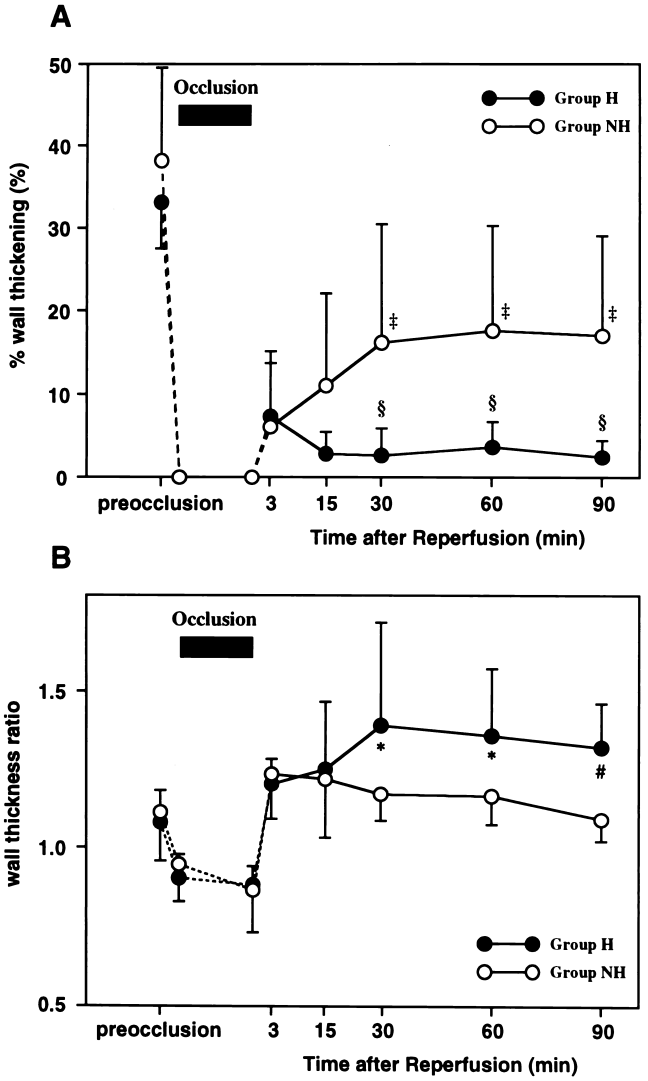

Figure 2. Line graphs comparing percent change in systolic wall thickening at risk area (**A**) and wall thickness ratio (**B**) between Group H and Group NH. In the period after reperfusion, systolic wall thickening was increased in Group NH, whereas it was unchanged in Group H. In both groups, wall thickness ratio at end-diastole was lower during coronary artery occlusion than before occlusion. This ratio recovered after reperfusion in Group NH, whereas it increased significantly at 30 min after reperfusion in Group H. Wall thickness ratio was significantly higher in Group H than in Group NH at 30, 60 and 90 min after reperfusion. *$p < 0.05$, #$p < 0.01$, §$p < 0.005$ versus Group NH. ‡$p < 0.005$ versus 3 min after reperfusion.

indicated that the contrast defect size at phases earlier than 15 min after reperfusion was smaller than the infarct size as a result of reactive hyperemia. Therefore, the existence of reactive hyperemia in all of our cases suggested that there was little microvascular disruption within the infarct area soon after reperfusion.

The contrast defect area increased with time after 15 min after reperfusion in Group H, whereas it was constant in Group NH. Necropsy revealed that the area of hemorrhage was almost the same as that of the contrast defect just before

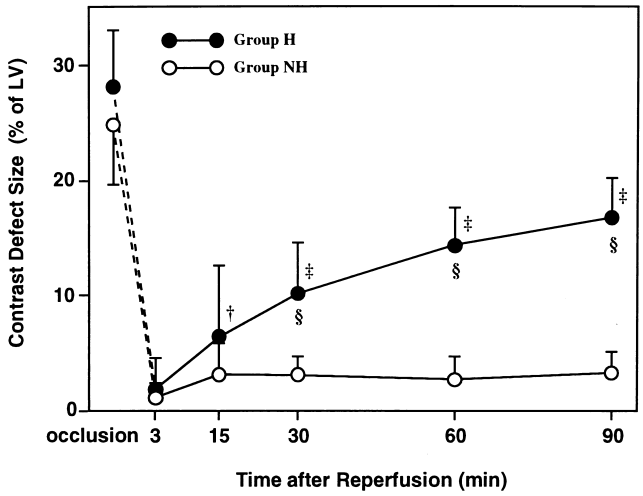

Figure 3. Line graph comparing contrast defect size determined by MCE in Group H and Group NH over time. In Group H, contrast defect size increased significantly from 3 to 90 min after reperfusion. There were significant differences between the two groups after 30 min after reperfusion. †$p < 0.05$, ‡$p < 0.005$ versus 3 min after reperfusion. §$p < 0.005$ versus Group NH. LV = left ventricle.

the dogs were euthanized. Expansion of contrast defect area may indicate progression of hemorrhage in reperfused areas. We speculate that there was a slight microvascular disruption soon after reperfusion and that capillaries either became occluded secondary to thrombus or microvascular spasm or were obstructed as a consequence of interstitial pressure elevation due to hemorrhage. As a result, the contrast defect area expanded gradually. Even in Group NH, which had no evidence of gross hemorrhage, there was a small degree of microvascular disruption with extravasation of erythrocytes into the interstitium histologically. However, it was difficult to identify these extravasations through observations of changes in wall thickness and the time-videointensity curves of MCE.

Time course of hemorrhage inferred from contrast defect after reperfusion. When does myocardial hemorrhage occur and how does it expand with time? Some investigators (17,29) have declared that the area of hemorrhage is smaller than that of myocardial necrosis, and that this hemorrhage is always within the necrotic area. Necrosis of myocytes would be completed and microvascular damage would have progressed during 3 h of coronary occlusion, and the injured capillaries would subsequently be disrupted after reperfusion (24,30,31). Cerra and co-workers (1) demonstrated that capillary disruption expanded transmurally during 180 min in a canine model. Gracia-Dorado et al. (24) demonstrated that the hemorrhage did not occur in a pig model subjected to 60 min of occlusion followed by 30 min of reperfusion and reocclusion, whereas definite hemorrhage was noted in pigs with prolonged reperfusion after 45 min of occlusion. In Group H, our study demonstrated development of an abnormally thickened wall detected at 30 to 60 min after reperfusion, indicating that myocardial hemorrhage occurred during that period.

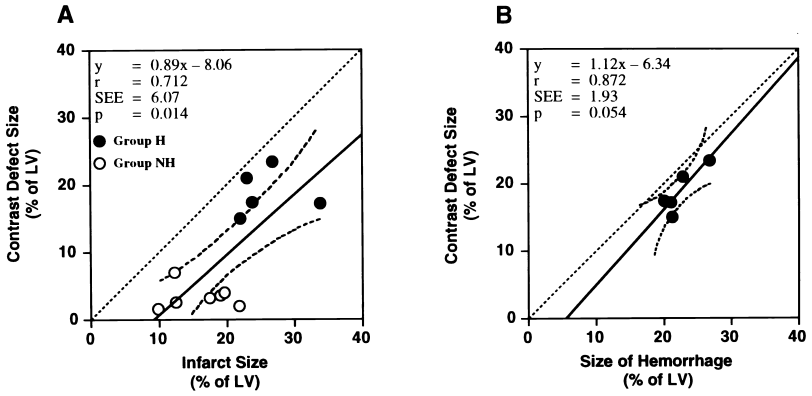

Figure 4. A, Relation between infarct size determined by hematoxylin-eosin staining (x axis) and echographic perfusion defect size (y axis) in the two groups. **B**, Relation between macroscopic hemorrhage size (x axis) and the perfusion defect size on MCE at 90 min after reperfusion (y axis) in Group H. **Dotted line** = the line of identity; **dashed curves** = 95% confidence limits of the regression line. LV = left ventricle.

No reflow and myocardial hemorrhage. Failure of recanalization of the microvasculature despite recanalization of larger vessels is referred to as a *no-reflow phenomenon* (32). Ito and co-workers (33) compared the findings of MCE with those of coronary angiography after reperfusion in patients with acute MI. They visually demonstrated the no-reflow phenomenon on MCE. Kloner (34) speculated that potential causes of the observed no-reflow phenomenon included several microscopic changes such as plugging of neutrophils or erythrocytes, contracture of microvasculature, swelling of the myocardium, endothelium damage and myocardial hemorrhage. It is difficult to specify the causes from clinical findings. Our present study demonstrated the significance of sequential measurements of wall thickness and contrast defect area after reperfusion. Both gradual thickening of the wall and extension of contrast defect area may be helpful in distinguishing hemorrhage from plugging of the microvasculature.

Limitations of the study. MCE has some limitations in evaluating myocardial perfusion quantitatively. Although we adjusted the gain settings of the equipment and the injection volume and speed of microbubbles throughout the experiment, these adjustments could not ensure that the density and size of microbubbles would be identical among injections and subjects. A large bubble mingling by chance with smaller ones will bias the washout time of the contrast echo to be long. In consideration of this possibility, we did not use the raw absolute data of our study, but rather compared the PI between the reperfused and remote areas. Fortunately, the border between opacified and nonopacified areas was clear and manual tracing of the border was easy. Tracings of the definite border were reproducible, even manually (18,35,36).

The definition of hemorrhage may be critical to interpretation of results. We classified subjects with microscopic but without gross hemorrhage as falling into the nonhemorrhage group (Group NH). Microscopic hemorrhage is very common in postischemic areas. The measurement of the area of hemorrhage is also critical. As discussed earlier, it would be difficult to quantify the size of microscopic hemorrhage because of patchy red cell extravasation and capillary degeneration, making the border zone unclear. In the present study, we measured the area of gross hemorrhage through the aid of photography, with which the border zone was relatively clearly defined.

Clinical implications. This study indicates that hemorrhagic MI may be diagnosed in the presence of combined

Figure 5. Same dog as in Figure 1. MCE at 90 min after reperfusion. **A**, Before injection of contrast agent. **B**, After injection. The extent of contrast defect (**arrows**) is similar to the area of hemorrhage in Figure 1.

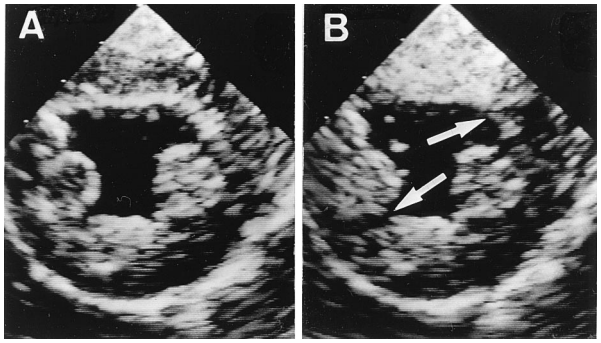

Figure 6. Line graph comparing the PI ratio of endocardium to epicardium on MCE between Group H and Group NH over time. In Group H, the serial changes of this ratio decreased significantly after reperfusion. There were significant differences between the two groups after 15 min of reperfusion. ‡$p < 0.005$ versus 3 min after reperfusion. §$p < 0.005$ versus Group NH.

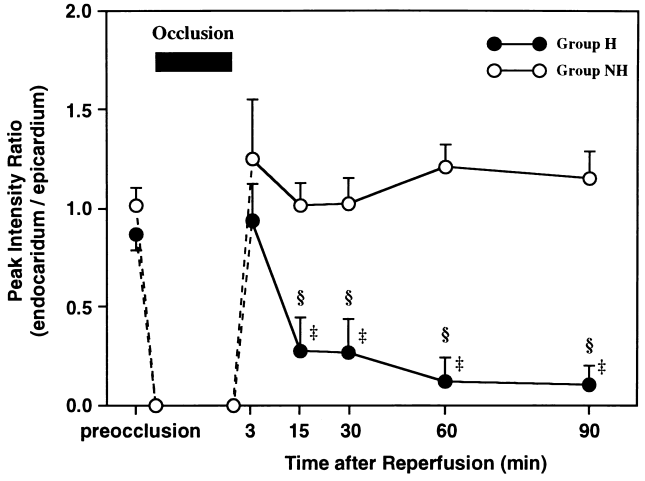

abnormal thickening of the reperfused region and extension of the perfusion defect after recanalization. Unfortunately, there is no method to diagnose hemorrhagic MI clinically at present, although the complication is a common clinical occurrence. With intravenous MCE (37–40), it is possible to observe myocardial perfusion repeatedly and noninvasively even in human studies, enabling the diagnosis of hemorrhagic MI after reperfusion therapy. We believe that our findings will help to reveal the mechanisms and prognosis of hemorrhagic MI.

We thank Joe Alexander, Jr., MD for valuable advice and careful checking of this report.

References

1. Cerra FB, Lajos TZ, Montes M, Siegel JH. Hemorrhagic infarction: a reperfusion injury following prolonged myocardial ischemic anoxia. Surgery 1975;78:95–104.
2. Kloner RA, Rude RE, Carlson N, Maroko PR, DeBoer LW, Braunwald E. Ultrastructural evidence of microvascular damage and myocardial cell injury after coronary occlusion: which comes first? Circulation 1980;62:945–52.
3. Kloner RA, Alker KJ. The effect of streptokinase on intramyocardial hemorrhage, infarct size, and the no-reflow phenomenon during coronary reperfusion. Circulation 1984;70:513–21.
4. Go LO, Murry CE, Richard VJ, Weischedel GR, Jennings RB, Reimer KA. Myocardial neutrophil accumulation during reperfusion after reversible or irreversible ischemic injury. Am J Physiol 1988;255:H1188–98.
5. Bolli R. Oxygen-derived free radicals and postischemic myocardial dysfunction (stunned myocardium). J Am Coll Cardiol 1989;12:239–49.
6. Krause SM, Jacobus WE, Becker LC. Alterations in cardiac sarcoplasmic reticulum calcium transport in the postischemic "stunned" myocardium. Circ Res 1989;65:526–30.
7. Przyklenk K, Kloner RA. "Reperfusion injury" by oxygen-derived free radicals?: effect of superoxide dismutase plus catalase, given at the time of reperfusion, on myocardial infarct size, contractile function, coronary microvasculature, and regional myocardial blood flow. Circ Res 1989;64:86–96.
8. Bolli R. Mechanism of myocardial "stunning." Circulation 1990;82:723–38.
9. Homeister JW, Hoff PT, Fletcher DD, Lucchesi BR. Combined adenosine and lidocaine administration limits myocardial reperfusion injury. Circulation 1990;82:595–608.
10. Pearson PJ, Schaff HV, Vanhoutte PM. Acute impairment of endothelium-dependent relaxations to aggregating platelets following reperfusion injury in canine coronary arteries. Circ Res 1990;67:385–93.
11. Marban E. Myocardial stunning and hibernation: the physiology behind the colloquialisms. Circulation 1991;83:681–8.
12. Hutchins GM, Bulkley BH. Infarct expansion versus extension: two different complications of myocardial infarction. Am J Cardiol 1978;41:1127–32.
13. Bresnahan GF, Roberts R, Shell WE, Ross JJ. Deleterious effects due to hemorrhage after myocardial reperfusion. Am J Cardiol 1974;33:82–6.
14. Lang TW, Corday E, Gold H, et al. Consequences of reperfusion after coronary occlusion: effects on hemodynamic and regional myocardial metabolic function. Am J Cardiol 1974;33:69–81.
15. Constantini C, Corday E, Lang TW, et al. Revascularization after 3 hours of coronary arterial occlusion: effects on regional cardiac metabolic function and infarct size. Am J Cardiol 1975;36:368–84.
16. Mathur VS, Guinn GA, Burris WH. Maximal revascularization (reperfusion) in intact conscious dogs, after 2 to 5 hours of coronary occlusion. Am J Cardiol 1975;36:252–61.
17. Fishbein MC, Y-Rit J, Lando U, Kanmatsuse K, Mercier JC, Ganz W. The relationship of vascular injury and myocardial hemorrhage to necrosis after reperfusion. Circulation 1980;62:1274–9.
18. Kaul S, Pandian NG, Okada RD, Pohost GM, Weyman AE. Contrast echocardiography in acute myocardial ischemia—I: in vivo determination of total left ventricular "area at risk." J Am Coll Cardiol 1984;4:1272–82.
19. Kemper AJ, O'Boyle JE, Cohen CA, Taylor A, Parisi AF. Hydrogen peroxide contrast echocardiography: quantification in vivo of myocardial risk area during coronary occlusion and of the necrotic area remaining after myocardial reperfusion. Circulation 1984;70:309–17.
20. Kaul S, Gillam LD, Weyman AE. Contrast echocardiography in acute myocardial ischemia—II: the effect of site of injection of contrast agent on the estimation of area at risk for necrosis after coronary occlusion. J Am Coll Cardiol 1985;6:825–30.
21. Kaul S, Glasheen W, Ruddy TD, Pandian NG, Weyman AE, Okada RD. The importance of defining left ventricular area at risk in vivo during acute myocardial infarction: an experimental evaluation with myocardial contrast two-dimensional echocardiography. Circulation 1987;75:1249–60.
22. Sakamaki T, Tei C, Meerbaum S, et al. Verification of myocardial contrast two-dimensional echocardiographic assessment of perfusion defects in ischemic myocardium. J Am Coll Cardiol 1984;3:34–8.
23. Vandenberg BF, Feinstein SB, Kieso RA, Hunt M, Kerber RE. Myocardial risk area and peak gray level measurement by contrast echocardiography: effect of microbubble size and concentration, injection rate, and coronary vasodilation. Am Heart J 1988;115:733–9.
24. Garcia-Dorado D, Theroux P, Solares J, Alonso J, et al. Determinants of hemorrhagic infarcts: histologic observations from experiments involving coronary occlusion, coronary reperfusion, and reocclusion. Am J Pathol 1990;137:301–11.
25. Murphy ML, Peng CF, Kane JJ, Straub KD. Ventricular performance and biochemical alteration of regional ischemic myocardium after reperfusion in the pig. Am J Cardiol 1982;50:821–8.
26. Haendchen RV, Corday E, Meerbaum S, Povzhitkov M, Rit J, Fishbein MC. Prevention of ischemic injury and early reperfusion derangements by hypothermic retroperfusion. J Am Coll Cardiol 1983;1:1067–80.
27. Haendchen RV, Corday E, Torres M, Maurer G, Fishbein MC, Meerbaum S. Increased regional end-diastolic wall thickness early after reperfusion: a sign of irreversibly damaged myocardium. J Am Coll Cardiol 1984;3:1444–53.
28. Villanueva FS, Glasheen WP, Sklenar J, Kaul S. Assessment of risk area during coronary occlusion and infarct size after reperfusion with myocardial contrast echocardiography using left and right atrial injections of contrast. Circulation 1993;88:596–604.
29. Roberts CS, Schoen FJ, Kloner RA. Effect of coronary reperfusion on myocardial hemorrhage and infarct healing. Am J Cardiol 1983;52:610–4.
30. Ganz W, Watanabe I, Kanamasa K, Yano J, Han DS, Fishbein MC. Dose reperfusion extend necrosis?: a study in a single territory of myocardial ischemia—half reperfused and half not reperfused. Circulation 1990;82:1020–33.
31. Farb A, Kolodgie FD, Jenkins M, Virmani R. Myocardial infarct extension during reperfusion after coronary artery occlusion: pathologic evidence. J Am Coll Cardiol 1993;21:1245–53.
32. Kloner RA. The "no-reflow" phenomenon after temporary coronary occlusion in the dog. J Clin Invest 1974;54:1496–508.
33. Ito H, Tomooka T, Sakai N, et al. Lack of myocardial perfusion immediately after successful thrombolysis: a predictor of poor recovery of left ventricular function in anterior myocardial infarction. Circulation 1992;85:1699–705.
34. Kloner RA. Does reperfusion injury exist in humans? J Am Coll Cardiol 1993;21:537–45.
35. Kemper AJ, Force T, Perkins L, Gilfoil M, Parisi AF. In vivo prediction of the transmural extent of experimental acute myocardial infarction using contrast echocardiography. J Am Coll Cardiol 1986;8:143–9.
36. Kaul S, Kelly P, Oliner JD, Glasheen WP, Keller MW, Watson DD. Assessment of regional myocardial blood flow with myocardial contrast two-dimensional echocardiography. J Am Coll Cardiol 1989;13:468–82.
37. Villanueva FS, Glasheen WP, Sklenar J, Jayaweera AR, Kaul S. Successful and reproducible myocardial opacification during two-dimensional echocardiography from right heart injection of contrast. Circulation 1992;85:1557–64.
38. Monaghan MJ, Metcalfe JM, Odunlami S, Waaler A, Jewitt DE. Digital radiofrequency echocardiography in the detection of myocardial contrast following intravenous administration of Albunex. Eur Heart J 1993;14:1200–9.
39. Skyba DM, Jayaweera AR, Goodman NC, Ismail GC, Kaul S. Quantification of myocardial perfusion with myocardial contrast echocardiography during left atrial injection of contrast: implications for venous injection. Circulation 1994;90:1513–21.
40. Dittrich HC, Bales GL, Kuvelas T, Hunt RM, McFerran BA, Greener Y. Myocardial contrast echocardiography in experimental coronary artery occlusion with a new intravenously administered contrast agent. J Am Soc Echocardiogr 1995;8:465–74.